

# On the Chirality of Self-Assembled DNA Octahedra\*\*

Yu He, Min Su, Ping-an Fang, Chuan Zhang, Alexander E. Ribbe, Wen Jiang, and Chengde Mao\*

Chirality is an essential aspect in nature.<sup>[1]</sup> Most biomolecules, such as amino acids, sugars, RNA, DNA, and proteins, are chiral, as are the large entities assembled from these molecules. The ability of enzymes and cell receptors to readily distinguish different stereoisomers (enantiomers) of chiral substrates leads to highly efficient and stereoselective reactions and binding. An understanding of and ability to control chirality is of crucial importance for organic synthesis,<sup>[2]</sup> molecular separation,<sup>[3]</sup> guest encapsulation,<sup>[4]</sup> drug design,<sup>[5]</sup> and other endeavors. In recent years, the exploration of biomimetic supramolecular self-assembly has provided a means to study the formation of chiral objects. This approach suggests a way to understand and control chirality at the molecular level. Previous studies mostly focused on the asymmetric assembly of nonbiological organic molecules through noncovalent interactions,<sup>[6–8]</sup> such as hydrogen bonds, metal coordination, or  $\pi$ – $\pi$  interactions. Herein, we report a well-defined chiral nanooctahedron structure which is exclusively composed of DNA molecules. The construction of the DNA octahedron involves a rather simple one-pot process involving only three unique synthetic DNA single strands. Cryogenic electron microscopy (cryoEM) revealed a three-dimensional (3D) structural map with a resolution of 12 Å, from which the chiral features of the DNA octahedron could be identified clearly.

DNA is a superb nanoscale building material owing to its excellent molecular-recognition capability and well-defined double-helical structure.<sup>[9]</sup> A variety of DNA nanostructures<sup>[10–13]</sup> have been engineered from synthetic DNA molecules. Since natural B-form DNA adopts a stereoisomerically pure right-handed double-helical structure, large DNA nanostructures can presumably also adopt chiral conformations. However, the chirality of DNA assemblies at the nanoscale

has rarely been investigated.<sup>[14,15]</sup> The chirality of DNA nanostructures arises from two aspects: 1) the intrinsic chirality of the DNA double helix and 2) overall geometric folding and association. Although the chirality of DNA duplexes is widely recognized, the geometric folding and association of component DNA molecules are not well-appreciated for their contribution to the chirality of the overall assemblies. One exception is a chiral DNA tetrahedron<sup>[14]</sup> reported by Turberfield and co-workers. The tetrahedral structure is composed of four unique single DNA strands, and each of its edges is a DNA duplex. Such DNA tetrahedra are stereoisomerically pure, presumably because the major grooves of the DNA tend to face inward at each vertex to minimize electrostatic interactions between the negatively charged DNA backbones. However, it remains a challenge to predict the chirality of DNA nanostructures. Herein, we report a well-defined 3D chiral DNA nanoobject, a DNA octahedron, whose chirality was clearly identified and can be explained by simple structural modeling.

A general strategy has recently been developed for the assembly of 3D DNA polyhedra.<sup>[16]</sup> This strategy relies on the self-limiting association of finite numbers of identical symmetrical DNA star motifs (tiles) and produces well-defined DNA tetrahedra, hexahedra (cubes), dodecahedra, icosahedra, and buckyballs. In such 3D assemblies, DNA tiles are bent from the tile plane. Bending in the two possible opposite directions results in pairs of enantiomers at the nanoscale. It is not clear whether these DNA polyhedra exist as equal mixtures of both enantiomers or are formed stereoselectively. In our previous study, we neglected this important question. In the current study, we used DNA octahedra to investigate this problem. Because they only contain triangular faces, octahedra are architecturally rigid and robust owing to the tensegrity principle. Such structural rigidity would greatly facilitate structural characterization and chirality investigations.

DNA octahedra were self-assembled from a previously developed symmetrical cross motif (four-point star; Figure 1). The basic DNA motif (tile), which has fourfold rotational symmetry, contains nine DNA strands but only three unique sequences.<sup>[17]</sup> The four component branches are identical and have pairs of complementary sticky ends at the peripheral termini. Each branch consists of two antiparallel pseudocontinuous DNA duplexes that are linked together by strand crossovers. With four five-base-long single-stranded loops at the center, the DNA tile is rather flexible; thus, the four branches can readily bend away from the tile plane. Through sticky-end association, DNA cross tiles can associate with each other and finally form closed polyhedral structures. Among such potential closed structures, an octahedron is the smallest stable structure that does not require bending of the rigid DNA duplexes. In each DNA octahedron, six identical

[\*] Y. He,<sup>[‡]</sup> C. Zhang, A. E. Ribbe, Prof. C. Mao  
Department of Chemistry, Purdue University  
West Lafayette, IN 47907 (USA)  
Fax: (1) 765-494-0239  
E-mail: mao@purdue.edu

M. Su,<sup>[‡]</sup> P.-A. Fang, Prof. W. Jiang  
Markey Center for Structural Biology and  
Department of Biological Sciences  
Purdue University, West Lafayette, IN 47907 (USA)

[‡] These authors contributed equally.

[\*\*] This research was supported by the Office of Naval Research (Award No. N000140910181). DLS studies were carried out in the Purdue Laboratory for Chemical Nanotechnology (PLCN). The cryoEM images were taken in the Purdue Biological Electron Microscopy Facility, and the Purdue Rosen Center for Advanced Computing (RCAC) provided the computational resources for the 3D reconstructions.

Supporting information for this article is available on the WWW under <http://dx.doi.org/10.1002/anie.200904513>.

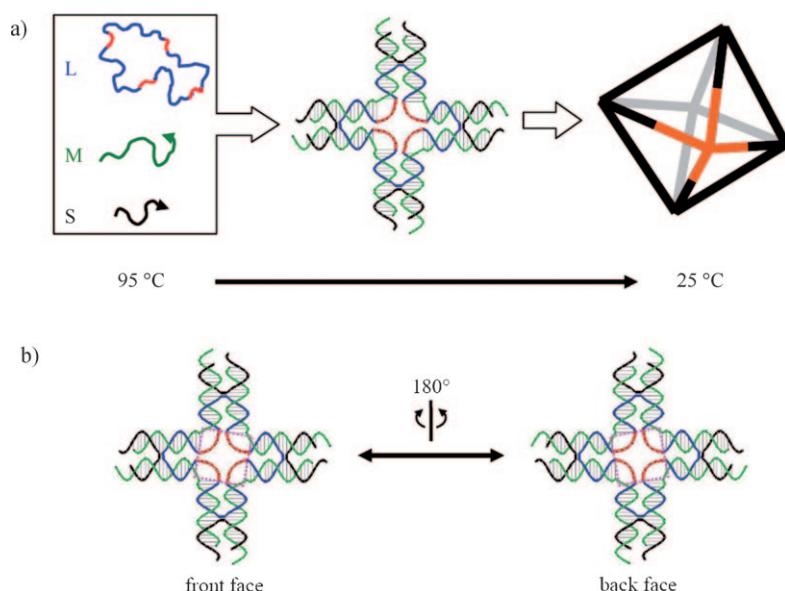


**Figure 1.** DNA octahedra. a) Schematic representation of the cooling-induced one-pot self-assembly of DNA octahedra from three unique DNA single strands: L, M, and S. Four short segments (red) in the L strand, which contains a sequence repeated four times, remain single-stranded at the center of the four-point-star intermediate tiles and in the final DNA octahedron. A four-point-star tile is highlighted in orange in the final octahedral structure. b) Two views of the central cavity of the four-point-star tile (from above and beneath the plane of the paper). The tile exposes its front or back face depending on whether the tile bends inward or outward, respectively. Note that the cavity is skewed in opposite directions in these two nanoscale isomers. The dashed boxes approximately delineate the central cavity as a guide to the eye.

symmetrical cross tiles are located at the vertices, and each edge is composed of two associated branches from two adjacent tiles.

The chirality of the DNA octahedra originates from out-of-plane bending (ca. 45°) by the component DNA tiles. Bending inward or outward from the plane results in pairs of isomeric, chiral octahedra (Figure 1b). The two possible isomers are mirror images at the nanometer scale if the DNA duplexes are considered as smooth rods. To distinguish the two possible conformations, we introduced a small geometric feature at the center of the tiles by purposely using slightly different strand lengths (10 and 11 base pairs) for the two component duplexes of each branch of the tile from the tile center to the crossover point. This length difference causes a relative skew between the square central cavity and the overall tetragonal geometry of the tile. Bending in opposite directions would position different faces (front or back) of the tiles to the outside of the octahedra and result in opposite skews as viewed from outside of the octahedra. Thus, the tile bending direction correlates with the relative skewing direction, which is observable experimentally by cryoEM imaging at a sufficiently high resolution. Note that the length difference between the two component duplexes generates an experimentally observable reporter for the octahedral chirality but is not the reason for the rise of chirality.

The DNA octahedra were assembled by previously reported methods.<sup>[16]</sup> Briefly, the three component DNA

single strands were mixed in the stoichiometric ratio (1:4:4) in a Tris-acetic acid-EDTA-Mg<sup>2+</sup> buffer (Tris = 2-amino-2-hydroxymethylpropane-1,3-diol, EDTA = ethylenediaminetetraacetic acid), and the mixture was slowly cooled from 95 to 25 °C over 1 h. The assembled DNA structures were characterized by a number of techniques, including nondenaturing polyacrylamide gel electrophoresis (PAGE), dynamic light scattering (DLS), atomic force microscopy (AFM), and cryoEM. Nondenaturing PAGE (see Figure S1 in the Supporting Information) indicated that the major assembly products contained six copies of the DNA four-point-star tile, a result consistent with an octahedral structure. By using ImageJ (an image-processing software developed by the National Institutes of Health), we estimated from the band intensity in the PAGE graph that the assembly yield was higher than 90% when the DNA-tile concentration was 150 nM or lower. DLS studies (see Figure S2 in the Supporting Information) revealed that the apparent hydrodynamic radius of the DNA complexes was (13.8 ± 1.9) nm, which agrees well with the radius of the circumscribed sphere of the expected DNA octahedron model (13.6 nm), if the standard B-DNA conformation is used (diameter: 2 nm; pitch: 0.33 nm per base pair). To visualize the assembled products, we used tapping-mode AFM imaging in air. Nearly uniform sized particles were distributed randomly on mica

surfaces (see Figure S3 in the Supporting Information). The particles had lateral dimensions of approximately 28–30 nm and a height of approximately 2.5 nm. These values are reasonable for the dehydrated and collapsed DNA octahedra. All of the above data suggested the formation of DNA octahedra with a high assembly yield.

We used cryoEM imaging followed by a single-particle 3D-reconstruction technique to investigate whether or not the DNA octahedra were chiral objects. This powerful technique in structural biology can be used to determine biomacromolecular structures under near-native conditions. For example, we used this technique previously to solve the structure of an icosahedral virus at near-atomic resolution.<sup>[18]</sup> In our previous studies, the best resolution was 25 Å for self-assembled DNA polyhedra (tetrahedra, cubes, dodecahedra, icosahedra, and buckyballs).<sup>[16]</sup> In the current study, we optimized the experimental conditions for the characterization of the DNA octahedra (Figure 2). In raw cryoEM micrographs of the DNA sample, many octahedral particles with the expected size (ca. 27 nm) were clearly visible. The application of the single-particle 3D-reconstruction technique to the observed particles gave an octahedral map at a resolution of 12 Å. This is among the highest reported resolution for rationally designed DNA nanostructures,<sup>[19]</sup> and a number of detailed features were revealed. First, each vertex of the octahedron contains a big cavity corresponding to the central cavity of the DNA tile. Each strut of the octahedron was

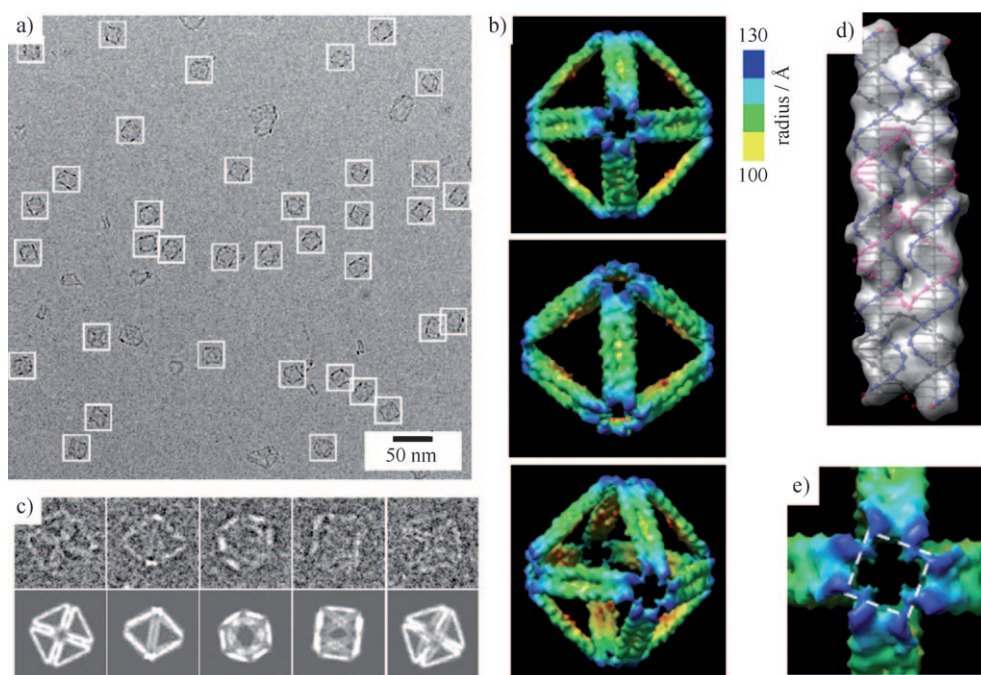


**Figure 2.** Analysis of the self-assembled DNA octahedra by cryogenic electron microscopy (cryoEM). a) A raw cryoEM image. b) Three views of the DNA octahedron reconstructed from DNA particles observed by cryoEM. The color gradient indicates the distance (radius) from the geometric center of the octahedron. c) Comparison of the raw images of an individual particle (top) with computer-generated 2D projections of the octahedral model (bottom) at similar orientations. d) View of a strut of the experimentally generated octahedral map superimposed on the structural model. e) Close-up view of a vertex of the DNA octahedral map. The dashed line approximately delineates the central cavity as a guide to the eye. The density maps in (b), (d), and (e) are from the reconstructed model.

shown as two parallel rods interconnected at two crossover points. The rods correspond to the two pseudocontinuous duplexes. The structural map obtained also hinted at right-handed helical conformations of the DNA duplexes in the central regions of the struts. The observation of a right-handed helical conformation could reasonably be expected for two-turn B-form DNA duplexes at 12 Å resolution. The intrinsic handedness of DNA helices served as an intrinsic reference for the overall chirality of the DNA octahedra. Second, the 3D structural map, as expected, showed a small shift in the positions of the parallel duplexes in each strut. When viewed from the outside of the DNA octahedra, the duplex that protrudes into the center is located on the right.

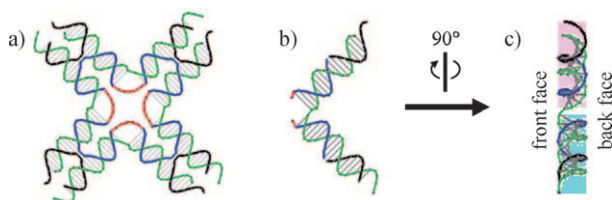


**Figure 3.** Detailed view of the two faces (front and back) of the four-point-star motif. For clarity, only one asymmetric segment is shown, and the middle three bases of the central, single-stranded loop are omitted. a) The DNA cross motif. b) Asymmetric segment of the cross tile (central region). c) The difference at the center between the two faces is responsible for the bending of the tile only towards the bottom face (inward).

The cavity square is skewed relative to the struts, and the skews can be observed easily in the structural model. This observation indicates that the DNA tiles bend inward. Thus, the self-assembly of the DNA octahedra is stereo-selective. It may be possible to use an electrophoresis-based method<sup>[20]</sup> that enables the quantitative analysis of bulk materials to determine the absolute ratio of the two isomers in a future study.

Why do the DNA tiles prefer to bend inward during assembly? To address this question, we carefully examined the structural model of the DNA cross motif (Figure 3). It is likely that only the central portion of the DNA tile influences the bending significantly. Thus, we focused our attention on that region. Figure 3b shows the asymmetric seg-

ment of the cross tile (only the central region). For clarity, the middle three bases of the central single-stranded loop are not shown. When this minimal structure is rotated by 90°, it becomes clear that the two faces of the structure are quite different in the central region. There is much more space at the back face than at the front face; thus, it is not surprising that the tile bends inward more readily than in the opposite direction. The same structural features are observed in other star-motif models (three-, five-, and six-point-star motifs).<sup>[16b,21]</sup> This observation prompts us to believe that the property of chirality is a general feature of all DNA polyhedra assembled by this strategy. However, this notion remains to be tested experimentally.

In summary, we have designed and assembled a chiral DNA octahedron. The assembly is rather straightforward and only involves three different synthetic DNA strands. A 3D structural map at 12 Å resolution helped to visualize the chirality features of the DNA octahedron. The chirality of DNA nanostructures is an important feature of well-defined DNA assemblies. We believe that DNA-templated nano-organization,<sup>[22]</sup> encapsulation,<sup>[23]</sup> and organic synthesis<sup>[24]</sup> could be controlled more precisely by taking advantage of the chirality of the DNA templates.<sup>[25]</sup>

Received: August 12, 2009

Revised: November 25, 2009

Published online: December 16, 2009



**Keywords:** chirality · DNA · nanostructures · self-assembly · supramolecular chemistry

- [1] W. J. Lough, I. W. Wainer, *Chirality in Natural and Applied Science*, CRC, Oxford, **2002**.
- [2] M. Lemaire, P. Mangeney, *Chiral Diazaligands for Asymmetric Synthesis*, Springer, Berlin, **2005**.
- [3] G. Gübitz, M. G. Schmid, *Chiral Separations: Methods and Protocols*, Humana, Totowa, NJ, **2004**.
- [4] J. Rebek, *Angew. Chem.* **2005**, *117*, 2104–2115; *Angew. Chem. Int. Ed.* **2005**, *44*, 2068–2078.
- [5] *Chiral Drugs* (Ed.: C. A. Challener), Wiley, Hampshire, England, **2001**.
- [6] L. R. MacGillivray, J. L. Atwood, *Nature* **1997**, *389*, 469–472.
- [7] L. J. Prins, J. Huskens, F. de Jong, P. Timmerman, D. N. Reinhoudt, *Nature* **1999**, *398*, 498–502.
- [8] L. J. Prins, F. de Jong, P. Timmerman, D. N. Reinhoudt, *Nature* **2000**, *408*, 181–184.
- [9] N. C. Seeman, *Nature* **2003**, *421*, 427–431.
- [10] U. Feldkamp, C. M. Niemeyer, *Angew. Chem.* **2006**, *118*, 1888–1910; *Angew. Chem. Int. Ed.* **2006**, *45*, 1856–1876.
- [11] F. C. Simmel, *Angew. Chem.* **2008**, *120*, 5968–5971; *Angew. Chem. Int. Ed.* **2008**, *47*, 5884–5887.
- [12] C. Lin, Y. Liu, S. Rinker, H. Yan, *ChemPhysChem* **2006**, *7*, 1641–1647.
- [13] F. A. Aldaye, A. L. Palmer, H. F. Sleiman, *Science* **2008**, *321*, 1795–1799.
- [14] J. C. Mitchell, J. R. Harris, J. Malo, J. Bath, A. J. Turberfield, *J. Am. Chem. Soc.* **2004**, *126*, 16342–16343.
- [15] R. P. Goodman, I. A. T. Schaap, C. F. Tardin, C. M. Erben, R. M. Berry, C. F. Schmidt, A. J. Turberfield, *Science* **2005**, *310*, 1661–1665.
- [16] a) Y. He, T. Ye, M. Su, C. Zhang, A. E. Ribbe, W. Jiang, C. Mao, *Nature* **2008**, *452*, 198–201; b) C. Zhang, M. Su, Y. He, X. Zhao, P. A. Fang, A. E. Ribbe, W. Jiang, C. Mao, *Proc. Natl. Acad. Sci. USA* **2008**, *105*, 10665–10669; c) C. Zhang, S. H. Ko, M. Su, Y. Leng, A. E. Ribbe, W. Jiang, C. Mao, *J. Am. Chem. Soc.* **2009**, *131*, 1413–1415.
- [17] Y. He, Y. Tian, Y. Chen, Z. Deng, A. E. Ribbe, C. Mao, *Angew. Chem.* **2005**, *117*, 6852–6854; *Angew. Chem. Int. Ed.* **2005**, *44*, 6694–6696.
- [18] W. Jiang, M. L. Baker, J. Jakana, P. Weigele, J. King, W. Chiu, *Nature* **2008**, *451*, 1130–1134.
- [19] T. Kato, R. P. Goodman, C. M. Erben, A. J. Turberfield, K. Namba, *Nano Lett.* **2009**, *9*, 2747–2750.
- [20] C. M. Erben, R. P. Goodman, A. J. Turberfield, *Angew. Chem.* **2006**, *118*, 7574–7577; *Angew. Chem. Int. Ed.* **2006**, *45*, 7414–7417.
- [21] a) Y. He, Y. Chen, H. Liu, A. E. Ribbe, C. Mao, *J. Am. Chem. Soc.* **2005**, *127*, 12202–12203; b) Y. He, Y. Tian, A. E. Ribbe, C. Mao, *J. Am. Chem. Soc.* **2006**, *128*, 15978–15979.
- [22] a) B. P. Duckworth, Y. Chen, J. W. Wollack, Y. Sham, J. D. Mueller, T. A. Taton, M. D. Distefano, *Angew. Chem.* **2007**, *119*, 8975–8978; *Angew. Chem. Int. Ed.* **2007**, *46*, 8819–8822; b) H. Yan, S. H. Park, G. Finkelstein, J. H. Reif, T. H. LaBean, *Science* **2003**, *301*, 1882–1884.
- [23] D. Bhatia, S. Mehtab, R. Krishnan, S. S. Indi, A. Basu, Y. Krishnan, *Angew. Chem.* **2009**, *121*, 4198–4201; *Angew. Chem. Int. Ed.* **2009**, *48*, 4134–4137.
- [24] X. Li, D. R. Liu, *Angew. Chem.* **2004**, *116*, 4956–4979; *Angew. Chem. Int. Ed.* **2004**, *43*, 4848–4870.
- [25] A. J. Mastroianni, S. A. Claridge, A. P. Alivisatos, *J. Am. Chem. Soc.* **2009**, *131*, 8455–8459.